E-Article

From Fine-Scale Foraging to Home Ranges: A Semivariance Approach to Identifying Movement Modes across Spatiotemporal Scales

Chris H. Fleming,[1,2,*] Justin M. Calabrese,[1,*,†] Thomas Mueller,[1,2] Kirk A. Olson,[1] Peter Leimgruber,[1] and William F. Fagan[2]

1. Smithsonian Conservation Biology Institute, National Zoological Park, Front Royal, Virginia 22630; 2. Department of Biology, University of Maryland, College Park, Maryland 20742; 3. Biodiversity and Climate Research Centre, Senckenberg Gesellschaft für Naturforschung, Senckenberganlage 25, 60325 Frankfurt (Main), Germany

Submitted May 2, 2013; Accepted October 10, 2013; Electronically published March 14, 2014

Online enhancement: zip file with appendixes. *Dryad data:* http://dx.doi.org/10.5061/dryad.45157.

ABSTRACT: Understanding animal movement is a key challenge in ecology and conservation biology. Relocation data often represent a complex mixture of different movement behaviors, and reliably decomposing this mix into its component parts is an unresolved problem in movement ecology. Traditional approaches, such as composite random walk models, require that the timescales characterizing the movement are all similar to the usually arbitrary data-sampling rate. Movement behaviors such as long-distance searching and fine-scale foraging, however, are often intermixed but operate on vastly different spatial and temporal scales. An approach that integrates the full sweep of movement behaviors across scales is currently lacking. Here we show how the semivariance function (SVF) of a stochastic movement process can both identify multiple movement modes and solve the sampling rate problem. We express a broad range of continuous-space, continuous-time stochastic movement models in terms of their SVFs, connect them to relocation data via variogram regression, and compare them using standard model selection techniques. We illustrate our approach using Mongolian gazelle relocation data and show that gazelle movement is characterized by ballistic foraging movements on a 6-h timescale, fast diffusive searching with a 10-week timescale, and asymptotic diffusion over longer timescales.

Keywords: autocorrelation function, characteristic timescales, continuous movement models, movement modes, semivariance function, variogram, variogram regression.

Introduction

Movement is a key process for many animal species that influences fitness via pathways ranging from foraging efficiency to mating success. Understanding why animals move and how they make movement decisions is therefore a fundamental problem in ecology (Mueller and Fagan 2008; Nathan et al. 2008). Movement is a complicated process that depends on an animal's internal state, its physiological constraints, and its environment, the outcome of which is a movement path consisting of a mixture of different movement behaviors (Schick et al. 2008; Gurarie et al. 2009). These various behaviors should leave statistically detectable signatures in movement paths (Morales et al. 2004; Gurarie et al. 2009), but decomposing that mixture into its component parts is a challenging task and an active area of research in movement ecology. As we describe in detail below, mixtures of movement behaviors occurring on markedly different spatiotemporal scales, such as small-scale foraging versus long-distance dispersal or migration, have proven especially difficult for current approaches to reliably tease apart.

Relocation data consist of repeated observations of the locations of individual animals, with observations typically collected at a constant sampling rate and thus separated by a fixed time interval. Current methods for identifying multiple movement behaviors, or movement modes, in such data sets proceed locally through each path (e.g., Morales et al. 2004; Jonsen et al. 2005; Gurarie et al. 2009; McClintock et al. 2012). It is assumed that the location data can be partitioned into sequences of steps corresponding to behavioral states, and transitions between these states are then identified and modeled as a function of environmental covariates.

Composite random walk models have been the main tools employed in analyses of multiple movement modes (Morales et al. 2004; Jonsen et al. 2005; McClintock et al. 2012). These models are built from mixtures of random walks (RWs), with each movement mode featuring its own

* These authors contributed equally to the work.
† Corresponding author; e-mail: calabresej@si.edu.

Am. Nat. 2014. Vol. 183, pp. E000–E000.
DOI: 10.1086/675504

set of parameters, together with a model describing transitions among modes. Composite RWs are typically fit to individual movement paths in a state-space framework (Jonsen et al. 2003, 2005; Patterson et al. 2008; McClintock et al. 2012). A recently developed alternative to composite RWs, behavioral change point analysis (BCPA; Gurarie et al. 2009), assumes that movement is a continuous-space, continuous-time stochastic process observed at discrete times. BCPA uses maximum likelihood to estimate the parameters governing this process within a moving window containing some number of adjacent movement steps. Portions of a path where parameter values change abruptly are identified as boundaries between different movement modes. Though BCPA is based on a continuous movement model, the likelihood function it employs is built by conditioning on differences between subsequent observations, thus imposing the data sampling rate on the underlying process model. Both composite RW and BCPA require estimating multiple parameters for each movement mode within a path and typically treat the paths of different animals separately (but see Jonsen et al. 2003), resulting in a potentially large number of parameters that must be estimated.

Methods that analyze movement paths step by step based on the sampling rate at which the data were collected—including simple RWs, composite RWs, and BCPA—require that the timescales governing the movement process are reasonably close to the sampling interval (see app. A [apps. A–F available online in the supplementary zip file] for a critique of RW models and demonstration of this issue with simulated data; Turchin 1998; Gautestad 2013). When this is the case, these methods are expected to produce reasonable results. However, it seems likely that this correspondence will often fail in real data, and it is difficult to check in practice. When the process and observation timescales differ substantially, these methods can yield highly biased results (Codling and Hill 2005), and if the data feature substantial gaps, then some movement modes may remain completely undetected (Breed et al. 2011). In other words, these approaches require an a priori choice of timescale, the sampling rate, on which the results depend sensitively. A simple example that pertains to our case study and typifies the source of this problem is given in figure 1. The key point is that time-lag-dependent phenomena such as diffusion need to be investigated and estimated with all possible time lags in the data, not only the sampling interval at which the data were collected. Despite repeated demonstrations of the severity of this issue (Bovet and Benhamou 1988; Turchin 1998; Codling and Hill 2005; Gautestad 2013), no widely accepted solutions exist and the problem is routinely ignored in practice. The sampling rate problem is further compounded for paths featuring mixtures of movements occurring on largely different spatiotemporal scales; even if the sampling rate is fortuitously close to one of the process timescales, it will likely not be close to the others. Appendix A.5 gives a clear demonstration of this behavior with simulated data.

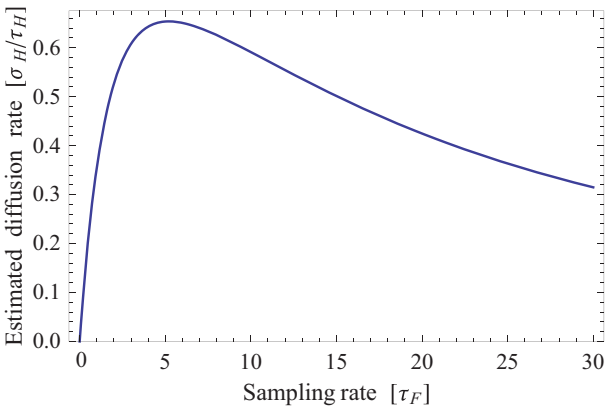

Figure 1: Conventionally estimated diffusion coefficient versus the sampling rate when the model is taken to be Brownian motion (BM), while the underlying process is actually the model of Ornstein–Uhlenbeck motion including foraging identified in the gazelle case study. The best result occurs when the sampling rate is in the regime wherein the BM model is most accurate, which occurs, in this case, where the diffusion-rate estimate peaks.

Here we show how the semivariance function (SVF) of a stochastic movement process offers both a novel approach to identifying multiple movement modes in relocation data and a solution to the sampling rate problem. The SVF contains equivalent information to the more familiar autocorrelation function (ACF), but the SVF is our focus here due to its superior statistical properties.[1] The SVF can be readily estimated from movement paths via variogram analysis (Cressie 1993), and the resulting variogram contains information on the mixture of movement modes present in a relocation data set. This approach uses all possible timescales (lags) in the data, not just the sampling interval. It is therefore inherently less sensitive to the particular choice of sampling rate than either composite RWs or BCPA, and it much more thoroughly uses the information in the data. The SVF can also be averaged over multiple animals in a relocation data set and over time when movement behavior is highly nonstationary, further increasing its statistical power.

We then describe how a family of continuous-space, continuous-time stochastic movement models represent-

[1] In particular, the SVF has unbiased estimators because it avoids directly estimating the mean and ordinary variance, for which the standard method-of-moments estimators are unreliable with autocorrelated data. Moreover, at any given time lag, the SVF is a simple χ^2 random variable when the underlying process is Gaussian, whereas the ACF is nonlinearly related to Student's *t*-distribution.

ing a wide range of behaviors can be expressed in terms of their SVFs, including simple random search (Brownian motion, BM), anomalous diffusion (AD), BM within a home range (Ornstein–Uhlenbeck motion, OU), and new models we introduce that generalize OU motion by including foraging (OUF). These models represent one (BM, AD), two (OU), or three (OUF) movement modes, with the most complicated among them completely described by only three parameters. The SVFs of these movement models can be fit to the empirical variogram via weighted least squares regression and then compared using standard model selection techniques to identify the mix of movement processes best supported by the relocation data. Focusing on Mongolian gazelles (*Procapra gutturosa*), we use these tools to reveal new insights about the different modes characterizing gazelle movement and the spatiotemporal scales on which these behaviors occur.

Methods

Fundamental Statistics of a Stochastic Movement Process

A relocation data set for an individual animal can be considered a realization of a stochastic process: a sequence of time-indexed random variables $x(t)$ that can be correlated in time. Just like random variables, stochastic processes can have moments or cumulants, and for many types of processes, these cumulants are fundamental statistics. For example, the widely applicable Gaussian stochastic process is entirely characterized by its first two cumulants, the mean and the positive-definite ACF or the negative-definite SVF (app. B; Abrahamsen 1997). For stationary Gaussian stochastic processes, which we assume here, the mean and the ACF/SVF are also constant in time. When observed velocity distributions, which can always be estimated from relocation data, are normally distributed about their mean, the mean and the SVF yield a complete description of animal motion. Notice that considering movement a Gaussian stochastic process is a very permissive assumption and can accommodate all of the movement models studied here, including anomalous diffusion, as well as many others. In other words, assuming a Gaussian stochastic process does not in any way restrict us to considering only Gaussian RWs (i.e., RWs with Gaussian step-length distributions) or Gaussian home-range areas (except for stationary processes).

The first cumulant, the nonstationary mean location $\mu(t) = \langle x(t) \rangle$, can reveal shifts in mean location over time. Such shifts could correspond to movement behaviors including seasonal migration and natal dispersal. However, our focus here is on cases that do not feature significant variation in the mean location over time, including movement within home ranges or territories, nomadic long-distance movements, or within-season nonmigratory movements of migratory animals. For such cases, a complete analysis need consider only the second cumulant (the ACF or, equivalently, the SVF) of the stochastic movement process.[2] The SVF $\gamma(t_1, t_2)$ measures the variability in the distance between two locations, $x(t_1)$ and $x(t_2)$, as a function of the time lag $\tau = t_2 - t_1$ between them and is calculated over all possible time lags in a data set. Plotting the estimated semivariance as a function of lag yields the empirical variogram, which contains information on the mix of processes represented in a relocation data set. In contrast, classical RW analyses focus on quantifying step-length distributions, turn-angle distributions, and comparing the observed mean squared displacement (MSD) to the model-predicted MSD (Turchin 1998; Codling et al. 2008). All of these quantities except the observed MSD are, however, sensitive to the usually arbitrary choice of sampling rate. Similarly, Nouvellet et al. (2009) showed how the turn-angle distribution is almost entirely determined by the sampling rate and how focusing on the ACF is more informative. When the SVF is estimated with confidence intervals, it contains the information of every possible step-length distribution (i.e., for all possible time lags in the data), and there is no need to guess at the relevant timescales of movement. On the other hand, while the empirical MSD is also insensitive to the sampling rate, its usual estimate (e.g., Turchin 1998) lacks the statistical reliability of SVF estimation, even though the two quantities correspond to the same statistical parameter for stationary processes such as diffusion. Therefore, when modeling diffusive and periodic behaviors, the SVF should generally be preferred over the MSD. In appendix sections A.1 and A.2, we compare both the step-length distribution and MSD to the SVF in more detail.

There are good methods for estimating autocorrelation structure other than the variogram, but we focus here on the variogram for two key reasons. First, the variogram is the only nonparametric autocorrelation estimator that, in appropriately modified form, could handle the kind of excessively gapped data that typify many animal tracking studies. Second, the variogram has a more familiar interpretation for ecologists, as it is very similar in nature to the MSD. If the data are more evenly sampled, the periodogram (Lomb 1976; Scargle 1982) estimates autocorrelation structure in the frequency domain and has the advantage of (relatively) uncorrelated errors, leading to better estimates of confidence intervals on model parameters (Fleming and Calabrese

[2] The SVF has the vast majority of the information in the ACF, except for the ordinary variance, and so the SVF is not entirely equivalent to the second cumulant. The SVF does, however, approach the ordinary variance asymptotically (for large lags). The advantage of avoiding direct estimates of the mean and ordinary variance is that the SVF has unbiased estimators, while the ACF does not.

2013). For analyzing nonstationary processes where the nonstationarity is of biological interest, time-frequency methods are appropriate but require very large data sets. Wavelet spectrograms are relatively easy to interpret and have been used before in movement ecology (Wittemyer et al. 2008; Polansky et al. 2010); however, only the Wigner-Ville function (Ville 1948; Hillery et al. 1984) is fully equivalent to the nonstationary autocorrelation function, which allows for more statistical flexibility such as population averaging. Finally, after the abovementioned nonparametric methods have been used to test and identify suitable movement models, maximum likelihood is by far the superior parameter estimation method (Fleming and Calabrese 2013). Its disadvantage is that it offers no way to visualize the autocorrelation structure of the data, which can be crucial for determining what class of models the data suggest (Auger-Methé et al. 2011). Given maximum likelihood's significant performance advantages, one might be inclined to directly use it to fit a set of candidate models to the data and then let Akaike Information Criterion (AIC) select the best model. However, this paper serves as a strong warning against such blind model selection, as the model that we found most consistent with the data is a completely new movement process that we identified only after visually noticing discrepancies between the variogram and existing movement models and then considering biologically motivated movement mechanisms that could produce an appropriate SVF.

SVF Estimation

Most methods of time-series analysis for estimating SVFs assume stationarity—that is, that the statistics of the stochastic process do not vary in time. Ecological systems subject to daily, seasonal, or annual cycles violate the stationarity assumption, and thus a nonstationary approach will typically be required when analyzing animal movement data. For a nonstationary process, the semivariance between times t_1 and t_2 depends not only on the lag, $\tau = t_2 - t_1$ but also on the absolute times. Our analysis effectively treats nonstationarity as a nuisance factor by first calculating the average time $\bar{t} = (t_1 + t_2)/2$ characterizing each pair of observations and then averaging over the dependence on $\bar{t}$, leaving only lag dependence. The resulting statistic is the time-averaged SVF, which contains equivalent information to the time-averaged ACF. Finally, as the semivariance estimate for an individual animal will be reliable for only the range of lags $dt < \tau \ll T$, where dt is the sampling time step and T is the sampling duration, we average the time-averaged SVF over individuals to improve the reliable range of lags up to $dt < \tau < T$, which allows us to robustly quantify movement over a wider range of timescales.

For evenly sampled data, the method-of-moments estimator of the SVF is

$$\hat{\gamma}(\tau) = \frac{1}{2n(\tau)} \sum_{\bar{t}} \left| x\left(\frac{\bar{t}+\tau}{2}\right) - x\left(\frac{\bar{t}-\tau}{2}\right) \right|^2, \qquad (1)$$

where $n(\tau)$ is the number of data pairs separated by lag τ, which are summed over in the time average. In brief, $\gamma(\tau)$ is the average squared distance between locations observed at two different times, where τ is the time lag separating the observations. This method of averaging over $\bar{t}$ is equivalent to the conventional method of averaging over all pairs of data with lag τ between them, but it reveals that for nonstationary processes this quantity represents a time-averaged summary of the full nonstationary semivariance (app. B). This reassures us that even if the data are significantly nonstationary, the standard method-of-moments estimator is still a meaningful quantity.

For data with many large, irregular gaps, such as the Mongolian gazelle data we analyze below or many marine mammal data sets in the literature (e.g., Jonsen et al. 2005; McClintock et al. 2012), we derive a new weighted variogram estimator that is also unbiased (app. B),

$$\hat{\gamma}(\tau) = \frac{\sum_{t_i - t_j = \tau} w_{ij} |x(t_i) - x(t_j)|^2}{2 \sum_{t_i - t_j = \tau} w_{ij}}, \qquad (2)$$

where the weights, w_{ij}, depend on the gap structure of the data and are given in appendix B. Plotting this statistic versus time lag gives the time- and individual-averaged (i.e., population) variogram, which serves as the basis for the rest of our analyses. To be meaningful, the population variogram requires a degree of similarity in movement behaviors among individuals, which, if the environment individuals experience is relatively similar, is reasonable to assume. For brevity, we will hereafter refer to this quantity simply as the variogram.

Though the variogram is much less sensitive to the details of data collection than conventional RW-based methods, both the sampling rate and the length of relocation time-series impose constraints on the underlying processes that can be detected. First, no method can detect a process occurring on a timescale shorter than the data sampling interval dt. Second, the upper limit on the process timescales that can be reliably identified is determined by the length of the time series T. Specifically, if the underlying process has a timescale τ_0, then the time series must span many times τ_0 to obtain a precise estimate of the semivariance for lags $\tau \geq \tau_0$. Within these constraints, however, no a priori assumptions need to be made about the important timescale(s) of a relocation data set, which is an important advantage over RW-based analyses. Finally, for (relatively) evenly sampled time-series data, the most re-

liable estimates of a variogram tend to be those at the shortest lags, because the number of observations used to estimate the semivariance tend to decrease with increasing lag. This means that the fine-scale features of the variogram occurring at small lags must be considered on equal or better footing to the more visually obvious large-scale features present for large lags. In fact, without the luxury of a population average, it is common to discard the latter half an individual variogram, as it can be so poorly behaved. As previously mentioned, the variogram contains information on the mix of movement processes in relocation data, and the SVF of a good movement model should therefore closely match the variogram across all lags (i.e., timescales) in the data.

SVFs of Alternative Movement Models

The next step in our analysis is to express movement models covering a wide range of movement behaviors in terms of their SVFs. In appendix C, we derive the SVFs (and hence ACFs) of a family of increasingly complex models, starting with simple Brownian motion. Here we present the ecological interpretation, SVF, and the parameters of each model.

BM: Regular Diffusion

BM describes a random search in a homogeneous area of infinite extent. Its SVF is given by

$$\gamma(\tau) = D|\tau| \tag{3}$$

(Gardiner and Gardiner 2009), where D is the diffusion rate. In this model, the SVF (and, equivalently, the MSD) increases without bound.

AD: Sub- and Superdiffusion

AD generalizes Brownian motion to power-law diffusion (Codling et al. 2008)

$$\gamma(\tau) = D_\alpha|\tau|^\alpha, \tag{4}$$

where $\alpha < 1$ corresponds to subdiffusion, $\alpha = 1$ corresponds to regular diffusion, and $\alpha > 1$ corresponds to superdiffusion. Unlike the other models considered here, there is no single derivation of AD that is generally applicable. Superdiffusion can arise when individuals move via a Levy-walk process, whereas subdiffusion can result from a combination of BM with barriers that impede movement (Codling et al. 2008). In particular, ballistic motion corresponds to $\alpha = 2$; as for any straight-line trajectory $x(t) = x_0 + v\,(t - t_0)$, we have the variance

$$|x(t + \tau) - x(t)|^2 = v^2|\tau|^2. \tag{5}$$

OU: BM within Home Ranges

The OU process generalizes Brownian motion by specifying a home range, σ_H, centered around a location, μ (Gardiner and Gardiner 2009). Within this area, the walker performs a random search for resources but with a central tendency to stay in the vicinity of μ. The SVF of OU motion is

$$\gamma(\tau) = \sigma_H\left(1 - e^{-|\tau|/\tau_H}\right), \tag{6}$$

where τ_H is the timescale associated with the animal covering its home range σ_H. The OU process is equivalent to the BM process in the limit of no central tendency, $\tau_H \to \infty$, and infinite range, $\sigma_H \to \infty$, with fixed diffusion rate $D = \sigma_H/\tau_H$. Outside of this limit, $D = \sigma_H/\tau_H$ is the diffusion rate for only small time differences relative to τ_H. In other words, the OU process represents a mix of regular (classical) diffusion over short timescales, $\tau < \tau_H$, and, due to the central tendency, asymptotes to a constant variance for longer time lags, $\tau > \tau_H$.

OUF: OU Motion with Foraging

Derived in appendix C, the generalized model we introduce here goes one step further and adds random foraging periods to the OU process. The OUF model includes a foraging timescale parameter, τ_F, which is the typical duration of a foraging bout. The OU model is recovered in the limit where there is no foraging, $\tau_F \to 0$. The three-parameter SVF under this model is given by

$$\gamma(\tau) = \sigma_H\left(1 - \frac{\tau_H e^{-|\tau|/\tau_H} - \tau_F e^{-|\tau|/\tau_F}}{\tau_H - \tau_F}\right), \tag{7}$$

where σ_H is the position variance, and τ_F and τ_H denote the relevant timescales. The behavior described by the OUF process is superdiffusive ($\alpha = 2$) for small time lags, $\tau < \tau_F$, given the Taylor expansion

$$\gamma(\tau) = \frac{\sigma_H}{2\tau_F\tau_H}|\tau|^2 + \mathcal{O}(|\tau|^3). \tag{8}$$

The behavior straightens to regular diffusion at intermediate timescales, $\tau_F < \tau < \tau_H$, and finally yields asymptotic diffusion over longer time periods, $\tau > \tau_H$.

In appendix C.4, we also considered modifying OU motion by including short timescale resting periods (OUR), which would look markedly different from OU motion in a fully nonstationary analysis. However, we prove in appendix C.4 that unlike OUF, an OUR process leaves no detectable signature in the short-lag part of the time-averaged variogram. In this short-lag regime, an OUR process will be indistinguishable from an OU process. Though there may be small differences between OUR and other

models for large lags, the variogram is too imprecise in this regime to reliably distinguish quantitatively similar models. We therefore did not attempt to fit the OUR model to the data and do not present its SVF here.

The BM and AD models assume the environment to be globally homogeneous and isotropic, while the OU and OUF models break this symmetry slightly by incorporating site fidelity. However, near the center of their home-range area, the OU and OUF models behave more like BM, and so they do assume a limited degree of spatial homogeneity and isotropy in their local environments.

SVF Parameter Estimation

To estimate the parameters of equations (3)–(7), we fit each to the population variogram via weighted least squares regression, which is similar to common practice in geostatistics (Cressie 1993). In our case, we used a number-weighted log least squares regression, adopted from periodogram analysis, which we found to be more reliable than the conventional variogram-weighted least squares regression (app. B.1). We then use AIC to select among these models and identify the mix of movement modes required to match the variogram. AIC is widely used in variogram regression (Cressie 1993); however, given the correlated nature of the variogram errors, AIC should not be used to select between qualitatively similar SVF models (Diggle and Ribeiro 2007). The variogram is not a complete summary of the data, so small AIC differences (or similarities) are not necessarily meaningful.

Mongolian Gazelle Case Study

We demonstrate the utility of these methods on GPS-collar data from 36 Mongolian gazelles tracked between 2007 and 2011. The data on which our analyses are based are deposited in the Dryad Digital Repository: http://dx.doi.org/10.5061/dryad.45157 (Fleming et al. 2014). Mongolian gazelles are found in the steppe and desert steppe habitats of eastern Mongolia and the border areas with China and Russia (Lhagvasuren and Milner-Gulland 1997; Wang et al. 1997). The study area is located on the Mongolian plateau, which consists of vast expanses of nearly flat grassland interspersed with low, rolling hills between 600 and 1,500 m in elevation. Outside of villages, humans are present at some of the lowest population densities in the world, and the population consists mostly of traditional pastoral herders moving between seasonal pastures (Olson et al. 2011).

We used gazelle relocation data collected in the eastern steppe of Mongolia using GPS-Argos collars (Telonics, Mesa, AZ). An example trajectory is given in figure 2. Sampling intervals varied among animals and ranged from 1 to 25 h. The GPS-Argos collars yielded relocations that were spatially very accurate but had gaps of various sizes because (*a*) the upload of GPS positions to Argos satellites occasionally failed, resulting in sporadic data loss, and (*b*) collars were programmed to have 10-day gaps after 5 days of data collection to extend the life of the battery. Overall, we used relocation data from 36 gazelles that were tracked from 50 to 917 days with a total of 8,111 relocations.

To demonstrate both the ability of our approach to recover the correct mix of processes and its overall robustness to sampling issues, we simulated movement paths (app. D) under the AIC-selected best model and performed the above-described analyses. We used a range of different sampling rates to check the robustness of our methods to the data sampling rate. We also simulated data sets that included the large, uneven gaps and mixed sampling rates typifying the gazelle data. Finally, we performed simulations with and without the observation error typical of the GPS collars used in the gazelle study. We quantified GPS location errors by using data from 15 gazelles that died during the study with their collars still on and functional. Most of these collars had a 1–3-m uncertainty, while two had a 20–30-m uncertainty. Relative to the scale of gazelle movement, these errors are negligible, but we included them in the simulations anyway to demonstrate that they do not meaningfully affect our results. However, when telemetry errors are substantial relative to the scale of movement, they can be incorporated into the SVF using the methods described in appendix C.5. All analyses were performed in Mathematica 8.0 (Wolfram Research, Champaign, IL).

Results

Our analysis identified three distinct movement behaviors in Mongolian gazelles that occurred across vastly different scales. Specifically, the OUF model, equation (7), was the only one that fit the entire variogram well, while the other models each missed at least one of the variogram's key features (fig. 3). The superiority of the OUF model is confirmed by AIC in table 1, as all other models have $\Delta\text{AIC} > 700$. The fact that the OUF model finds such overwhelming support in the data is strong evidence for the existence of three distinct movement modes for gazelles.

For intermediate lags, there is a roughly linear increase in semivariance with lag, consistent with classical BM. All four models are capable of describing this feature of the variogram, at least in isolation. Examining the ends of the variogram, however, reveals why the OUF model fits so much better than the others. For large lags, the semivariance reaches an asymptote, and only the OU and OUF models can accommodate the transition from BM at in-

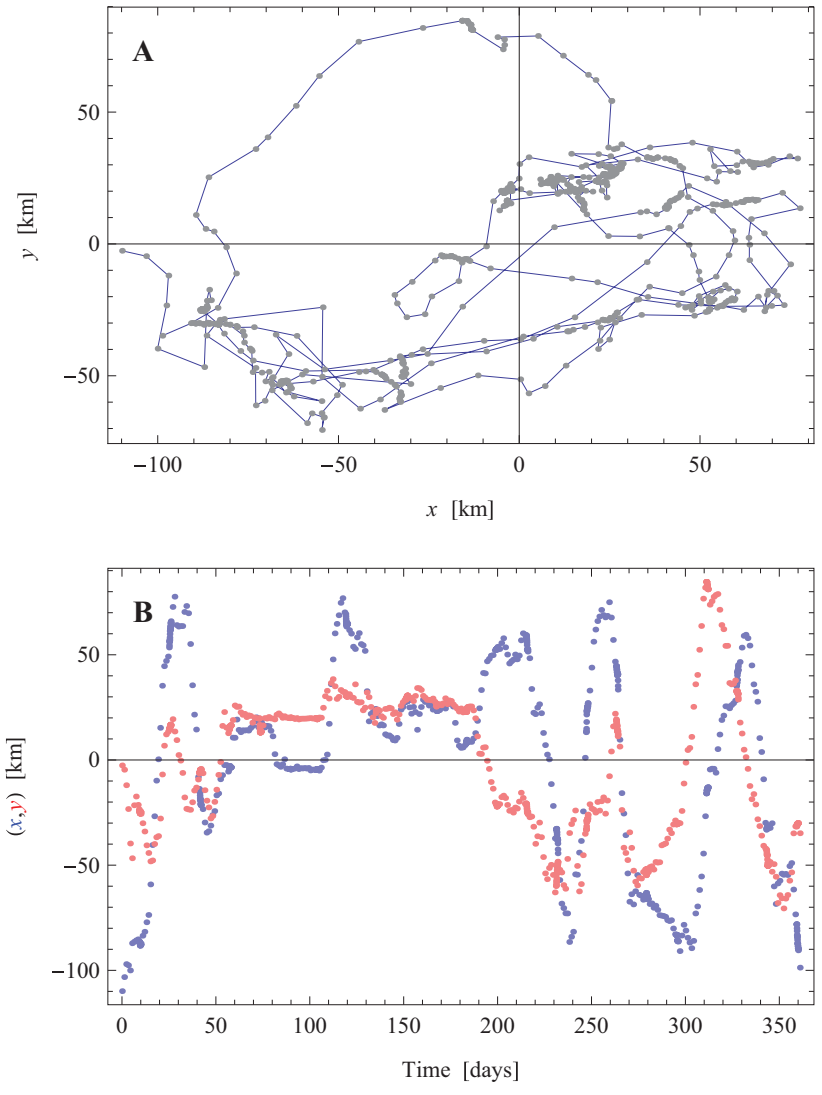

Figure 2: Spaghetti plot of the linearly interpolated raw locations (*A*) and relocations as a function of time (*B*) for the single best gazelle time series. Note that the sampling is highly uneven. It is difficult to distinguish movement scales and behaviors from either of these representations of an individual's trajectory. The variogram is essentially a means of visualizing time-lag-dependent behaviors in the data and thus much more informative to look at.

termediate lags to asymptotic diffusion at large lags (fig. 3). Zooming in on the small-lag end of the variogram, there is an initial convex portion that describes the transition from a lack of diffusion at very short lags to the above-noted approximately linear increase in semivariance with lag for intermediate lags (fig. 4*A*). The OUF model captures this transition, whereas the OU model produces only BM at the shortest lags and thus cannot simultaneously describe both the small and intermediate lag portions of the variogram (fig. 4). It is important to remember here that the shortest lags represent the most reliable semivariance estimates, so this fine-scale feature of the variogram cannot simply be ignored.

The OUF model parameter estimates we obtained from weighted least squares regression are given in figure 5. Under this model, the average Mongolian gazelle has two well-defined timescales in its motion: a short timescale of 6.16 ± 0.58 h and a long timescale of 74.1 ± 3.6 days. These timescales correspond to different residence (or range) length scales of $\ell_F = 4.09 \pm 0.48$ km and $\ell_H = 69.4 \pm 8.2$ km. These characteristic time and length scales describe the transitions among the three different types of diffusive behavior noted above and are shown for reference in figure 4.

A detailed picture of gazelle movement emerges from this analysis. For short time lags $t < \tau_F \approx 6$ h, the gazelles

confine themselves to a small region of approximately $\ell_F \approx 4$ km in extent, exhibiting only small movements. This is a period of anomalous diffusion consistent with individuals tracing relatively straight (i.e., ballistic) paths, as would be the case when an ungulate grazes (Bailey et al. 1996). At intermediate time lags, $\tau_F < t < \tau_H$, the gazelle exhibit classical BM. This period should correspond to a random search throughout a fairly homogeneous distribution of good habitat areas (each roughly ℓ_F in extent). Finally, for longer time lags, $t > \tau_H$, the diffusion rate slows down exponentially. Extrapolating the best-fit model predicts that the area covered would eventually peak, corresponding to a well-defined asymptotic range and yielding a range estimate of 91,000 ± 21,000 km^2 (fig. 5). As gazelles transition from regular to asymptotic diffusion on a timescale of $\tau_H \approx 10$ weeks, which is a fraction of a year, the asymptotic range is comparable to the gazelles' yearly range.

Our remaining results focus on confirming our key assumptions and demonstrating the robustness of our approach to sampling issues. When the velocity estimates from all individuals are overlaid, they conform well to the Gaussian assumption on which our approach is based (fig. 6*A*). Furthermore, the mean velocities in both the x (fig. 6*B*) and y (fig. 6*C*) directions exhibit no deterministic trends over time and are consistently within error of zero.

Table 1: Akaike Information Criterion (AIC) differences from weighted least squares fits of the semivariance functions of our movement models to the variogram

Model	ΔAIC
Brownian motion (BM)	1,174
Anomalous diffusion	1,098
BM + home range (Ornstein–Uhlenbeck motion, OU)	705
OU + foraging (OUF)	0

Note: For reproduction purposes, the (minimum) AIC of the OUF model was found to be 2,216.

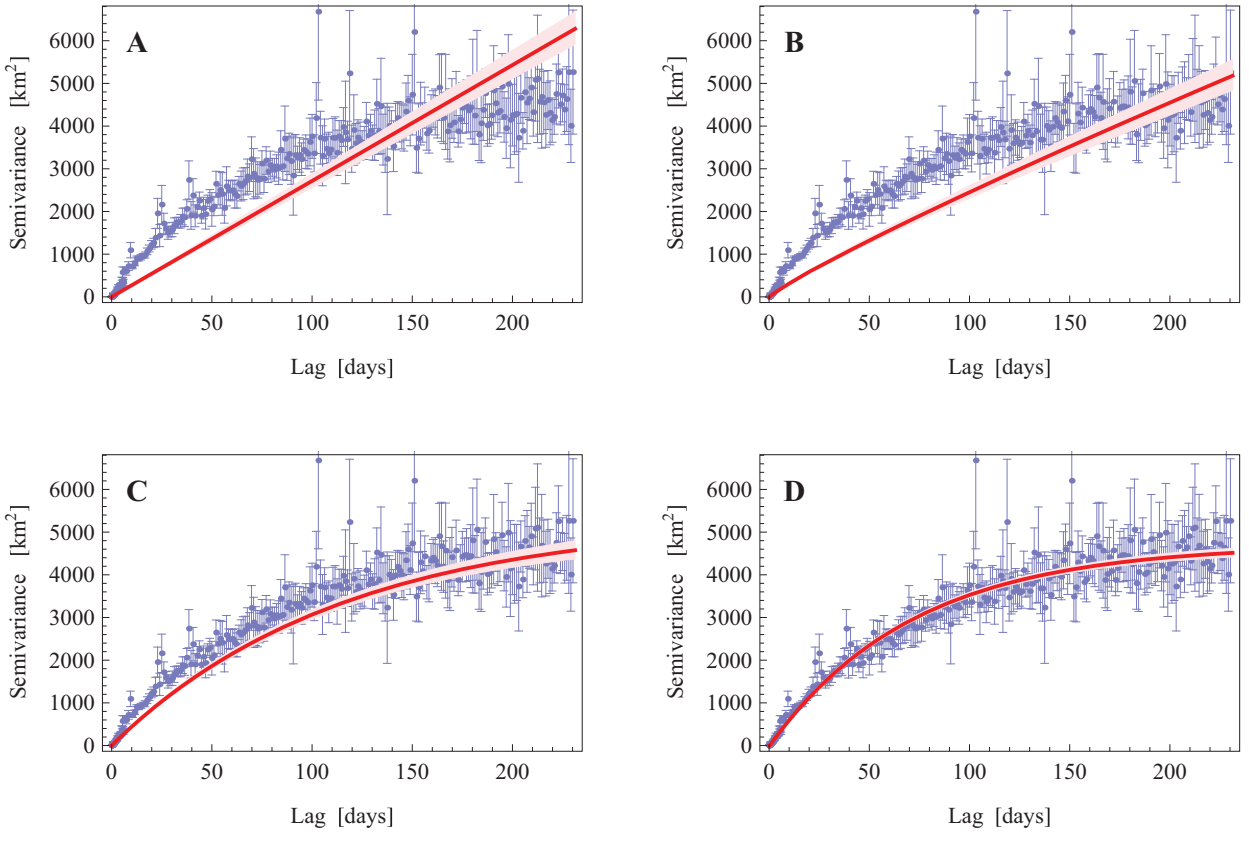

Figure 3: Comparison of the fitted movement models (red curves) to the variogram (blue): Brownian motion (*A*), anomalous diffusion (power law, *B*), Brownian motion with home range (Ornstein–Uhlenbeck motion, *C*), and Ornstein–Uhlenbeck with foraging (*D*). Semivariance estimates are accompanied by 95% confidence intervals estimated from the standard error of the mean semivariance, while the shaded regions around the best-fit models are 95% confidence intervals estimated from the standard error of the best fit.

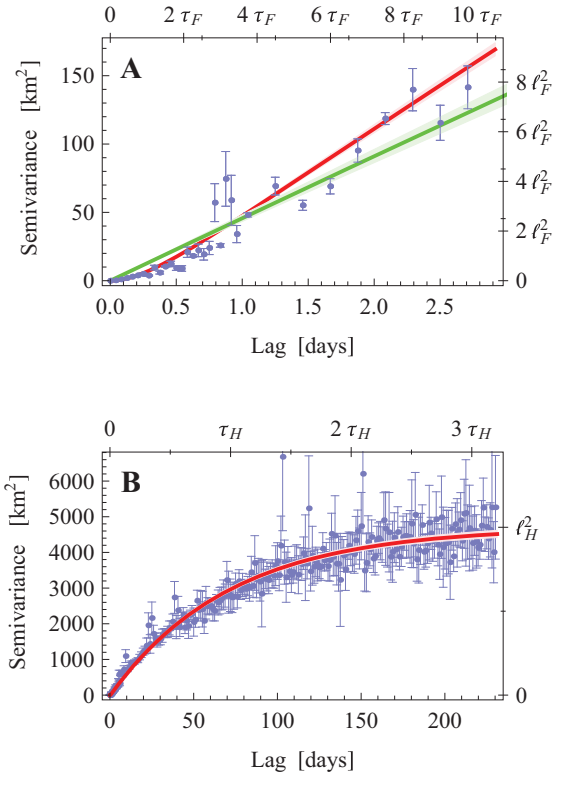

Figure 4: Fit of the Ornstein–Uhlenbeck with foraging (OUF) model to the variogram, with the estimated time and length scales displayed on the top and right frame edges, respectively. *A*, The small-lag behavior of the variogram (blue) with the best fit Ornstein–Uhlenbeck (green) and OUF (red) models. The short time and length scales (τ_F and ℓ_F) are displayed for reference. *B*, The overall fit of the OUF model with the long time and length scales (τ_H and ℓ_H) for reference. For both panels, the shaded regions around the best-fit models are 95% confidence intervals estimated from the standard error of the best fit, and the blue error bars around the semivariance estimates are 95% confidence intervals estimated from the standard error of the mean semivariance.

These observations justify both our assumption of a Gaussian stochastic process and our exclusive focus on the SVF.

The variogram calculated from data simulated from the OUF model with the parameter values in figure 5 looks qualitatively similar to the gazelle variogram, with the three different diffusive regimes clearly visible (fig. 7*A*, 7*B*). Notice that the data were simulated such that the extremely uneven sampling of the real gazelle data was reproduced. This analysis thus suggests that our major results were not artifacts of the highly gapped nature of the gazelle data. However, simulations where the sampling was even in time demonstrate that dramatic improvements in semivariance estimates and the corresponding SVF fits are possible, even when 75% of the observations are randomly deleted (fig. 7*C*, 7*D*). Fitting the OUF model to the simulated data produces parameter estimates similar to the parameter values that generated the data; however, the estimates were biased due the fact that the combination of inconsistent sampling schedules and individual movement variability forced us to standardize the individual time series before combining them in the population variogram (fig. 5; app. E.3).

Discussion

We have described a new and widely applicable framework for analyzing animal relocation data and robustly identifying multiple movement modes. Our approach employs a family of continuous-space, continuous-time movement models that cover a diverse range of behaviors. We write these models in terms of their SVFs and then couple them to relocation data via individual- and time-averaged variogram analysis. This novel approach allows us to seamlessly integrate fine- and broadscale movement behaviors in the same framework and to identify the mix of processes necessary to thoroughly describe a relocation data set.

When applied to Mongolian gazelles, our analysis has provided strong evidence for three distinct movement modes ranging from fine-scale foraging behavior all the way up to annual range. Our results suggest that gazelle movement consists of ballistic movement at short timescales that, on zooming out in lag, appears diffusive at intermediate timescales and increasingly subdiffusive over longer timescales. We hypothesize that the short-timescale regime corresponds to grazing or foraging behavior, with ℓ_F delimiting the size of the typical foraging area and τ_F describing the typical time required to exploit that area. Given that $\tau_F < 1$ day, it was conceivable that this movement mode could have been an artifact of either diurnal (i.e., periodic) resting behavior, such as sleeping during parts of the night, or randomly interspersed resting periods, as might occur after gazelles have foraged and need to ruminate. However, we prove in appendix C.4 that neither periodic nor random resting behaviors can produce the small-lag anomalous diffusion present in the variogram, even though resting behaviors might occur on a similar subdaily timescale. These resting behaviors modify the diffusion rate but not the qualitative behavior of the time-averaged SVF, and so they will not leave a detectable signature in the variogram (app. C.4). Instead, this small-lag behavior is an important feature of gazelle movement that would have likely remained undetected in a conventional composite RW analysis due to the gaps in the gazelle data (10 days) being many times longer than the timescale (≈6 h) over which this behavior occurs (Breed et al. 2011).

Over intermediate timescales, gazelles perform relatively unoriented movements that are well approximated by classical BM. These movements slow down for longer lags

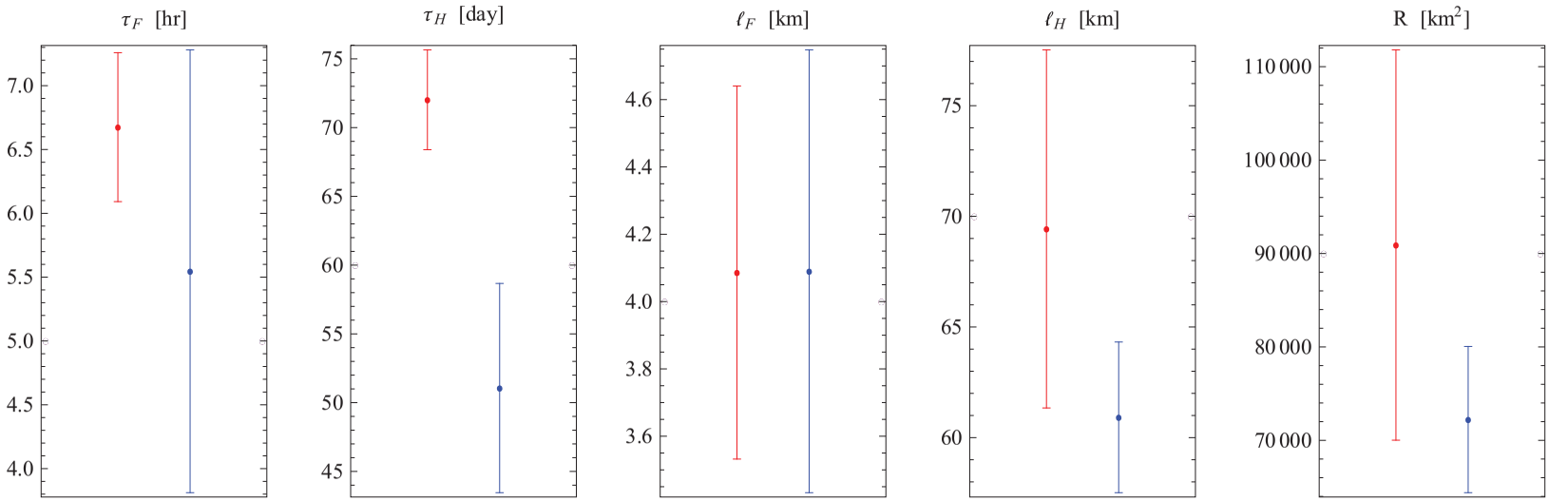

Figure 5: Best-fit parameters for the gazelle data in red, along with results of a parametric bootstrap in blue, where 300 simulated data sets (app. D; apps. A–F available in the supplementary zip file, available online) generated from the best fit were fitted back to the model. The length scales are given by $\ell_F = \sqrt{\tau_F/\tau_H \ell_H}$ and $\ell_H = \sqrt{\sigma_H}$, while the ranging area is given by $R = 2.45^2 \pi \ell_H^2$, where the factor of 2.45 is the approximate ninety-fifth percentile point of the bivariate standard normal distribution in one direction. Significant bias in the larger parameter estimates is a result of being forced to standardize the data because of data quality issues (app. E.3).

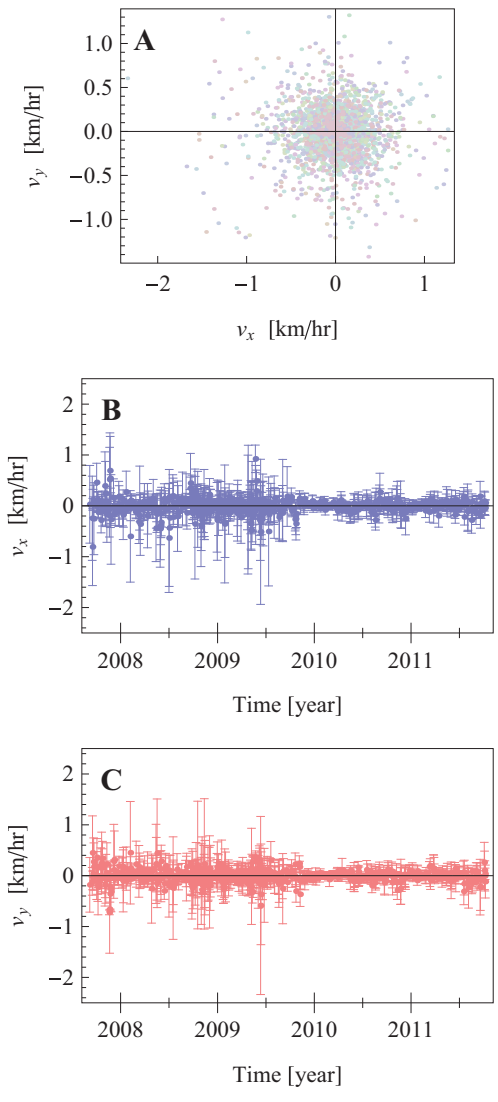

Figure 6: *A*, Distribution of velocities is roughly Gaussian, which justifies our assumption of gazelle movement conforming to a Gaussian process and indicates that we need only consider the mean and semivariance function (SVF). Additionally, the population average of the velocities over time in both the x (*B*) and y (*C*) directions is largely within error of zero, with no apparent deterministic trends. The lack of temporal trend in mean velocity allows us to consider the mean to be a static quantity for each animal. Taken together, these results indicate that basing our analysis entirely on the SVF is appropriate for the gazelle data.

such that individuals remain in large but well-defined areas. In terms of the foraging hypothesis outlined above, this movement behavior might be a random search for areas of good forage, with individuals remaining within one larger cluster of such areas. This interpretation suggests the testable hypothesis that the length scales characterizing foraging areas and clusters of foraging areas in the vegetation should correspond to the characteristic length scales of gazelle movement. The normalized difference vegetation index (NDVI) has been shown to be a good predictor of gazelle presence and gazelle movement (Mueller et al. 2008, 2011); therefore, a future analysis of the autocorrelation structure of NDVI data should allow this hypothesis to be examined more thoroughly.

The asymptotic range estimate of 91,000 ± 21,000 km^2—roughly the size of Portugal and more than three times the size of the Serengeti-Mara ecosystem—is substantially larger than previous estimates based on minimum convex polygons for single gazelles (14,700–32,300 km^2; Olson et al. 2010) and highlights the extremely large area requirements of Mongolian gazelles. Our estimates are bigger than those in the literature for two reasons. First, home-range estimators that ignore autocorrelation in movement data, such as minimum convex polygons and kernel density estimators, can be expected to consistently produce underestimates of home-range size (see app. F). Second, some of this discrepancy with previous results is due to the much larger and longer-term data set on which the new estimates are based. It is important to note, however, that none of our gazelle relocation time series lasted more than 2 years. Given that median female gazelle age is 4 years (Olson et al. 2014), it is possible that range estimates would increase even further over longer time spans. If this were to happen, it would imply movement behavior different from that captured by the OUF model over timescales longer than 2 years. These enormous area requirements support conservation concerns over fenced borders and transportation infrastructure such as the Trans-Mongolian Railway that act as barriers to gazelle movement. The range estimate reported in this study is the best estimate of Mongolian gazelle area requirements in the Eastern Steppe to date, as past estimates employ ad hoc home-range estimation methods that ignore autocorrelation in the movement data (see below) and are based on much smaller data sets (Olson et al. 2010) or report only annual distance moved (Berger 2004; Ito et al. 2006; Mueller et al. 2011).

Compared to ad hoc home-range estimation methods such as minimum convex polygons and kernel density estimators, a key advantage of our asymptotic range estimate, which it shares with mechanistic home-range analysis (Moorcroft and Lewis 2006; Moorcroft et al. 2006; Börger et al. 2008), is that it is derived from a mechanistic movement model. However, our approach does not require as detailed an understanding of the behaviors defining home ranges as mechanistic home-range analysis but instead relies on identifying movement mechanisms that are consistent with the full autocorrelation structure of the data.

In comparison to existing techniques for identifying

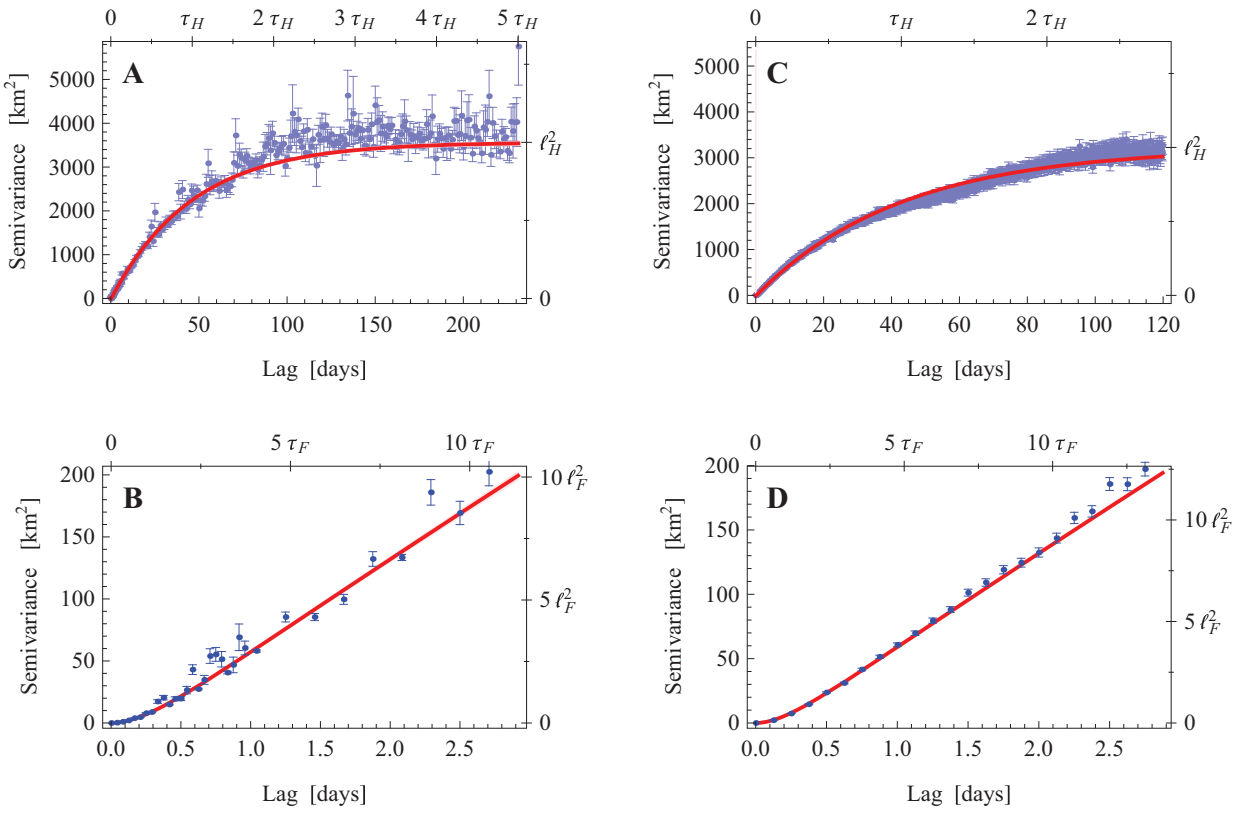

Figure 7: *A*, *B*, Simulated data from the best-fit Ornstein–Uhlenbeck with foraging (OUF) model with the larger (20–30 m) GPS location errors and the same degree of gapping as the real gazelle data. Compare to figure 4, which was estimated from the real gazelle data. The variogram calculated from the simulated data recovers all of the movement modes present in the OUF model, and fitting the OUF model back to the simulated data returns reasonable, though negatively biased parameter estimates from the standardization. *C*, *D*, Simulated gazelle data from the best-fit OUF model with the larger GPS errors, but with a sampling schedule of $dt = 2.5$ h and $T = 150$ days and with 75% of the observations randomly deleted, simulating a high measurement failure rate. This sampling regime barely encompasses the relevant timescales of the OUF process that generated the data, with the highest resolution being only $\approx\tau_F/2$ and the time series duration being $\approx 2\ \tau_H$. This analysis highlights the ability of our methods to identify the characteristic timescales of a movement data set, provided those timescales fall reasonably within the data sampling regime. Despite the high failure rate, the relative quality of the variogram and corresponding OUF fit, as compared to the severely gapped simulations depicted in *A*, *B*, demonstrates the dramatic improvements that are possible when regular sampling intervals are used.

movement modes such as composite RWs or BCPA, our approach has fewer parameters, uses more of the information in the data, is substantially less sensitive to the data sampling rate, and can deal with severely gapped, nonstationary data sets. The sampling rate problem inherent in all analyses based on location differences between observations (e.g., RW, composite RW, and BCPA) is intrinsically related to the scale dependence of animal movement. This long-standing issue can be resolved only by an approach that is equivalent to examining the autocorrelation at all possible timescales in the data. This feature of our SVF-based method, coupled with the parameter sparseness of our models, yields more reliable identification of multiple movement modes than existing techniques. Furthermore, the robustness of our method to gapped data is particularly attractive for movement analyses of hard-to-track species, such as marine mammals (e.g., Jonsen et al. 2005; McClintock et al. 2012). In contrast, composite RW methods are often unable to identify movement modes that occur over timescales shorter than the average length of data gaps (Breed et al. 2011).

A potential limitation of our framework for heavily gapped data combined with pronounced individual variability is that the individual time series may need to be standardized before pooling, which can result in a biased population variogram and biased SVF parameter estimates (fig. 5; app. E.3). For better data, where standardization and pooling are not required, the conventional and weighted variograms are unbiased, and there are several choices of unbiased regression methods (app. B.1). This

potential for bias is, however, a small price to pay given that our method still performs reasonably where current techniques break down (see app. A.5). Even sampling results in major improvements in semivariance estimates and SVF parameter estimates (cf. fig. 7*A*, 7*B* and fig. 7*C*, 7*D*) and is thus strongly recommended. An unavoidable limitation of our framework is that variogram regression techniques ignore the fact that the variogram itself has correlated errors, and so variogram regressions have a strong tendency to underestimate confidence intervals on SVF parameters in large data sets, even though the point estimates may be unbiased and relatively accurate (Fleming and Calabrese 2013). Going a step further, using maximum likelihood to fit an ACF directly to movement data would completely solve these estimation problems, but this approach brings with it additional computational challenges and also requires that one has already identified a good ACF/SVF model (Fleming and Calabrese 2013). To facilitate model identification, we strongly recommend that any lag-based movement analysis begin with a nonparametric estimator of the autocorrelation structure of the data that can be visualized, such as the variogram or the periodogram.

A potential advantage of composite RW and BCPA relative to our framework is that one can associate transitions between movement modes with environmental covariates. It is important to realize, however, that these methods associate segments of a movement path with a particular movement mode, and when the underlying process timescales are substantially different than the data sampling rate, this correspondence might break down. Inferences about the relationships between environmental covariates and movement modes may thus be unreliable. Relating transitions among movement modes to covariates would be difficult to accomplish via variogram regression because individual time series would need to be broken into pieces, and the pieces would likely be too small to produce reliable variograms. However, a full maximum likelihood ACF analysis could, in principle, accommodate environmental covariates.

Finally, Gurarie and Ovaskainen (2011) have recently shown that a broad range of stochastic movement models produced very similar emergent behavior once their characteristic timescales and length scales were aligned. They suggested that characteristic scales could serve as a model-independent common currency for describing and understanding movement. While their analysis focused on models with a single timescale and a single length scale (like the OU model), they proposed exploring how well their ideas generalize to models with multiple characteristic scales (like our OUF model). However, methods to estimate multiple characteristic scales have been lacking. Our approach, particularly when focusing on the OUF model introduced here or extensions of it, could serve to fill this gap.

Acknowledgments

We thank S. Bewick for helpful comments on the manuscript and J. Blanke for sharing his composite RW code. We are also grateful to the Ministry of Environment and Green Development of Mongolia for granting permission to capture and collar gazelles. This work was supported by National Science Foundation grants ABI-1062411, DEB-0743385, and DEB-0743557.

Literature Cited

Abrahamsen, P. 1997. A review of Gaussian random fields and correlation functions. Norwegian Computing Center, Oslo.

Auger-Methé, M., C. C. St. Clair, M. A. Lewis, and A. E. Derocher. 2011. Sampling rate and misidentification of Lévy and non-Lévy movement paths: comment. Ecology 92:1699–1701.

Bailey, D. W., J. E. Gross, E. A. Laca, L. R. Rittenhouse, M. B. Coughenour, D. M. Swift, and P. L. Sims. 1996. Mechanisms that result in large herbivore grazing distribution patterns. Journal of Range Management 49:386–400.

Berger, J. 2004. The last mile: how to sustain long-distance migration in mammals. Conservation Biology 18:320–331.

Börger, L., B. D. Dalziel, and J. M. Fryxell. 2008. Are there general mechanisms of animal home range behaviour? a review and prospects for future research. Ecology Letters 11:637–650.

Bovet, P., and S. Benhamou. 1988. Spatial analysis of animals' movements using a correlated random walk model. Journal of Theoretical Biology 131:419–433.

Breed, G. A., D. P. Costa, M. E. Goebel, and P. W. Robinson. 2011. Electronic tracking tag programming is critical to data collection for behavioral time-series analysis. Ecosphere 2:art10.

Codling, E. A., and N. A. Hill. 2005. Sampling rate effects on measurements of correlated and biased random walks. Journal of Theoretical Biology 233:573–588.

Codling, E. A., M. J. Plank, and S. Benhamou. 2008. Random walk models in biology. Journal of the Royal Society Interface 5:813–834.

Cressie, N. 1993. Statistics for spatial data. Revised edition. Wiley, New York.

Diggle, P. J., and P. J. Ribeiro. 2007. Model-based geostatistics. Springer, New York.

Fleming, C. H., and J. M. Calabrese. 2013. On the estimators of autocorrelation function parameters. Preprint arXiv:1301.4968.

Fleming, C. H., J. M. Calabrese, T. Mueller, K. A. Olson, P. Leimgruber, and W. F. Fagan. 2014. Data from: From fine-scale foraging to home ranges: a semivariance approach to identifying movement modes across spatiotemporal scales. American Naturalist, Dryad Digital Repository, http://dx.doi.org/10.5061/dryad.45157.

Gardiner, C. W., and C. Gardiner. 2009. Stochastic methods: a handbook for the natural and social sciences. Vol. 4. Springer, Berlin.

Gautestad, A. 2013. Animal space use: distinguishing a two-level

superposition of scale-specific walks from scale-free Lévy walk. Oikos 122:612–620.
Gurarie, E., R. D. Andrews, and K. L. Laidre. 2009. A novel method for identifying behavioural changes in animal movement data. Ecology Letters 12:395–408.
Gurarie, E., and O. Ovaskainen. 2011. Characteristic spatial and temporal scales unify models of animal movement. American Naturalist 178:113–123.
Hillery, M., R. F. O'Connell, M. O. Scully, and E. P. Wigner. 1984. Distribution functions in physics: fundamentals. Physics Report 106:121–167.
Ito, T. Y., N. Miura, B. Lhagvasuren, D. Enkhbileg, S. Takatsuki, A. Tsunekawa, and Z. Jiang. 2006. Satellite tracking of Mongolian gazelles (*Procapra gutturosa*) and habitat shifts in their seasonal ranges. Journal of Zoology 269:291–298.
Jonsen, I. D., J. M. Flemming, and R. A. Myers. 2005. Robust state-space modeling of animal movement data. Ecology 86:2874–2880.
Jonsen, I. D., R. A. Myers, and J. M. Flemming. 2003. Meta-analysis of animal movement using state-space models. Ecology 84:3055–3063.
Lhagvasuren, B., and E. J. Milner-Gulland. 1997. The status and management of the Mongolian gazelle *Procapra gutturosa* population. Oryx 31:127–134.
Lomb, N. R. 1976. Least-squares frequency analysis of unequally spaced data. Astrophysics and Space Science 39:447–462.
McClintock, B. T., R. King, L. Thomas, J. Matthiopoulos, B. J. McConnell, and J. M. Morales. 2012. A general discrete-time modeling framework for animal movement using multistate random walks. Ecological Monographs 82:335–349.
Moorcroft, P., and M. A. Lewis. 2006. Mechanistic home range analysis. Vol. 43. Princeton University Press, Princeton, NJ.
Moorcroft, P. R., M. A. Lewis, and R. L. Crabtree. 2006. Mechanistic home range models capture spatial patterns and dynamics of coyote territories in Yellowstone. Proceedings of the Royal Society B: Biological Sciences 273:1651–1659.
Morales, J., D. Haydon, J. Frair, K. Holsinger, and J. Fryxell. 2004. Extracting more out of relocation data: building movement models as mixtures of random walks. Ecology 85:2436–2445.
Mueller, T., and W. Fagan. 2008. Search and navigation in dynamic environments: from individual behaviors to population distributions. Oikos 117:654–664.
Mueller, T., K. A. Olson, G. Dressler, P. Leimgruber, T. K. Fuller, C. Nicolson, A. J. Novaro, et al. 2011. How landscape dynamics link individual- to population-level movement patterns: a multispecies comparison of ungulate relocation data. Global Ecology and Biogeography 20:683–694.
Mueller, T., K. A. Olson, T. K. Fuller, G. B. Schaller, M. G. Murray, and P. Leimgruber. 2008. In search of forage: predicting dynamic habitats of Mongolian gazelles using satellite-based estimates of vegetation productivity. Journal of Applied Ecology 45:649–658.
Nathan, R., W. M. Getz, E. Revilla, M. Holyoak, R. Kadmon, D. Saltz, and P. E. Smouse. 2008. A movement ecology paradigm for unifying organismal movement research. Proceedings of the National Academy of Sciences of the USA 105:19052–19059.
Nouvellet, P., J. P. Bacon, and D. Waxman. 2009. Fundamental insights into the random movement of animals from a single distance-related statistic. American Naturalist 174:506–514.
Olson, K. A., T. K. Fuller, T. Mueller, M. G. Murray, C. Nicolson, D. Odonkhuu, S. Bolortsetseg, and G. B. Schaller. 2010. Annual movements of Mongolian gazelles: nomads in the Eastern Steppe. Journal of Arid Environments 74:1435–1442.
Olson, K. A., E. A. Larsen, T. Mueller, P. Leimgruber, T. K. Fuller, G. B. Schaller, and W. F. Fagan. 2014. Survival probabilities of adult Mongolian gazelles using continuous-time telemetry-based survival analysis. Journal of Wildlife Management 78:35–41.
Olson, K. A., T. Mueller, J. T. Kerby, S. Bolortsetseg, P. Leimgruber, C. R. Nicolson, and T. K. Fuller. 2011. Death by a thousand huts? effects of household presence on density and distribution of Mongolian gazelles. Conservation Letters 4:304–312.
Patterson, T. A., L. Thomas, C. Wilcox, O. Ovaskainen, and J. Matthiopoulos. 2008. State-space models of individual animal movement. Trends in Ecology and Evolution 23:87–94.
Polansky, L., G. Wittemyer, P. C. Cross, C. J. Tambling, and W. M. Getz. 2010. From moonlight to movement and synchronized randomness: Fourier and wavelet analyses of animal location time series data. Ecology 91:1506–1518.
Scargle, J. D. 1982. Studies in astronomical time series analysis. II. Statistical aspects of spectral analysis of unevenly spaced data. Astrophysical Journal 263:835–853.
Schick, R. S., S. R. Loarie, F. Colchero, B. D. Best, A. Boustany, D. A. Conde, P. N. Halpin, L. N. Joppa, C. M. McClellan, and J. S. Clark. 2008. Understanding movement data and movement processes: current and emerging directions. Ecology Letters 11:1338–1350.
Turchin, P. 1998. Quantitative analysis of movement: measuring and modeling population redistribution in animals and plants. Sinauer, Sunderland, MA.
Ville, J. 1948. Théorie et applications de la notion de signal analytique. Câbles et Transmission 2:61–74.
Wang, X., H. Sheng, J. Bi, and M. Li. 1997. Recent history and status of the Mongolian gazelle in Inner Mongolia, China. Oryx 31:120–126.
Wittemyer, G., L. Polansky, I. Douglas-Hamilton, and W. M. Getz. 2008. Disentangling the effects of forage, social rank, and risk on movement autocorrelation of elephants using Fourier and wavelet analyses. Proceedings of the National Academy of Sciences of the USA 105:19108–19113.

Associate Editor: Benjamin Bolker
Editor: Judith L. Bronstein